PHYSICAL REVIEW E **68**, 025202(R) (2003)

Experimental Chua-plasma phase synchronization of chaos

Epaminondas Rosa, Jr.,[1,2] Catalin M. Ticos,[2,3] William B. Pardo,[2] Jonathan A. Walkenstein,[2] Marco Monti,[2] and Jürgen Kurths[4]

[1]*Department of Physics, Illinois State University, Normal, Illinois 61790-4567, USA*

[2]*Nonlinear Dynamics Laboratory, Department of Physics, University of Miami, Coral Gables, Florida 33146, USA*

[3]*Engineering Science, University of Oxford, Parks Road, Oxford OX1 3PJ, United Kingdom*

[4]*Nonlinear Dynamics, Institute of Physics, University of Potsdam, D-14415 Potsdam, Germany*

(Received 18 December 2002; published 26 August 2003)

Experimental phase synchronization of chaos is demonstrated for two different chaotic oscillators: a plasma discharge and the Chua circuit. Our technique includes real-time capability for observing synchronization-desynchronization transitions. This capability results from a strong combination of synchronization and control, and allows tuning adjustments for search and stabilization of synchronous states. A power law is observed for the mean time between 2π phase slips for different coupling strenghts. The experimental results are consistent with the numerical simulations.

DOI: 10.1103/PhysRevE.68.025202 PACS number(s): 05.45.Gg, 05.45.Pq, 05.45.Xt

The recurrence property of chaotic flows suggests that the corresponding flow trajectories can, in general, be viewed as an infinite number of rotational motions. In the particular situation where these rotational motions go around a fixed axis, an angle coordinate can be introduced as a state space variable and be regarded as the oscillator's phase. For example, in the case of a chaotic trajectory going around the z axis, we can define the phase on the (x,y) projection of the attractor as $\phi=\arcsin(y/r)$ where $r=\sqrt{x^2+y^2}$. This phase can synchronize with the phase of a periodic forcing function properly connected to the chaotic system [1]. The phase synchronous state then is characterized by the chaotic and the periodic oscillators having their phases in pace with each other, while keeping their amplitudes uncorrelated [2]. Phase synchronization of chaos has been extensively demonstrated [3], including chaotic plasmas forced with a periodic wave function [4], and with a music signal [5]. Moreover, the experimental effect of additive noise on phase synchronization, associated with chaotic transients has been the subject of recent investigation [6].

In this paper we report experimental and numerical phase synchronization results involving a plasma discharge tube coupled to a Chua electronic circuit. We introduce a technique for real-time observation and control of experimental synchronization. To our knowledge this is the first experimental realization of phase synchronization between two very different experimental chaotic oscillators, in association with supporting numerical results. The setup of our experiment is shown in Fig. 1. It includes the Chua circuit [7] with $R=1025\Omega$, $C_1=10$ nF, $C_2=133$ nF, $L=21.5$ mH, and $r_0=10\ \Omega$. This circuit is unidirectionally coupled to a plasma circuit through a LM 741 operational amplifier and a current limiting resistor R_c. The plasma circuit contains a commercial Geissler discharge tube filled with helium gas. The driving signal from the Chua circuit is the voltage across the capacitor C_1. The coupling strength is controlled by the variable resistor R_c in the range from 30Ω to 5 kΩ. A ballast resistor $R_b=49$ kΩ sustains the tube discharge while the resistor $R_0=2$ kΩ provides a low potential point in the circuit ($V_A\sim 3$ V), where the voltage driving signal from the Chua circuit is introduced. A stabilized high voltage source set at $E=916$ V is used to power the discharge. A *p-i-n* photodiode is utilized for acquiring the local light intensity oscillations of the plasma discharge at the positive column. Time delay embedding is then applied to the acquired light signal to produce the plasma attractor.

The attractor obtained from the dynamical trajectory of the chaotic plasma discharge resembles a smeared circle [4], continually circulating around its center. Both plasma and Chua oscillators are phase coherent and exhibit broad power spectra with a predominant characteristic frequency. In the beginning of the experimental run, the characteristic frequencies of the two uncoupled oscillators are far apart from each other. Prior to coupling the two systems, we tune the Chua oscillator to make its characteristic frequency approach the value of the characteristic frequency of the plasma. This feature of the setup enhances the synchronization process, and can be used for controlling purposes after the coupling is turned on. It works as follows. On the screen of the computer

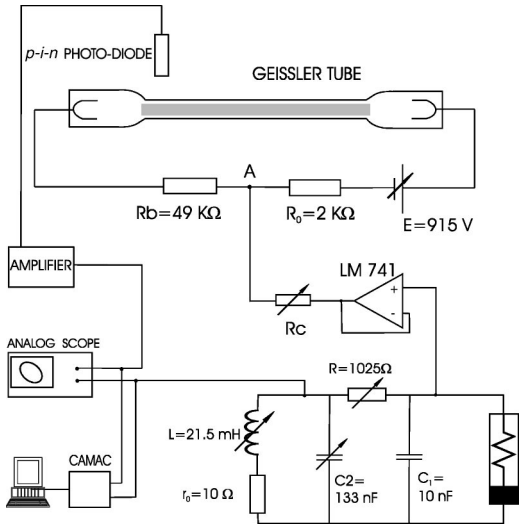

FIG. 1. Schematic representation of the Chua-plasma experimental setup.

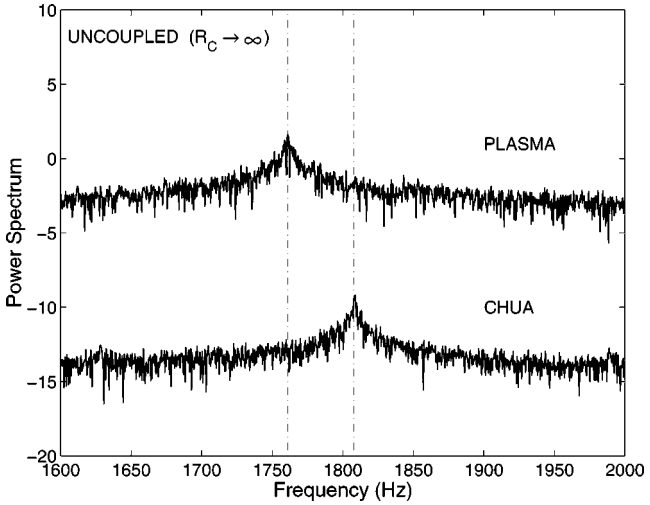

FIG. 2. Power spectra of the uncoupled plasma and of the Chua oscillator. Notice the small mismatch between the dominant frequencies.

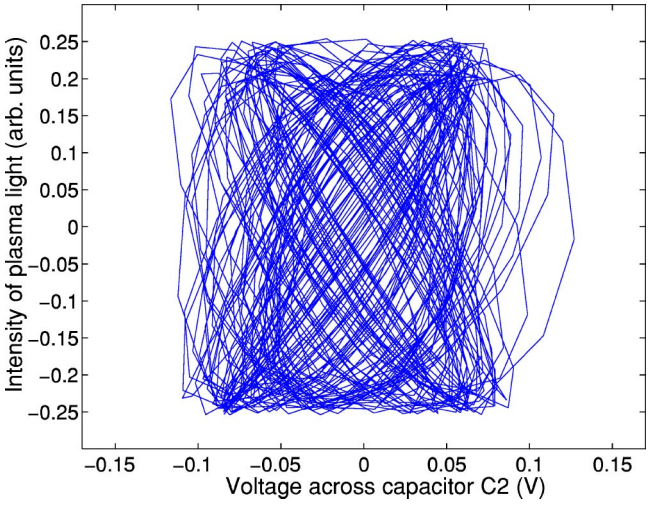

FIG. 3. Plot of the voltage across capacitor C_2 of the Chua circuit vs the light intensity of the plasma discharge when the two oscillators are not coupled.

we plot the power spectra of both oscillators. These power spectra are obtained from time series acquired with a computer automated measurement and control Lecroy 6810 wave form recorder, and acquisition period adjusted to $T_s = 50\ \mu$s. The recorded data sets contain 2.62×10^5 points which account for about 13.1 s of continuous monitoring of the two systems. Initially the peaks of the power spectra of the two oscillators are far apart, as expected, since the oscillators are running independent of each other. To make the characteristic frequency f_{Chua} approach the characteristic frequency of the plasma f_{plasma}, we have the options of three variable parameters: the resistance R, the capacitor C_2, and the inductor L (see Fig. 1). These three variable parameters, with corresponding reference values of $R=2\ \text{K}\Omega$, $C_2 = 100$ nF, and $L=18$ mH [7], allow a smooth change of the dynamics of the Chua oscillator. The other capacitor is set at $C_1=10$ nF and kept unchanged. We fix R at 1025 $\text{K}\Omega$, and slowly increase C_2 and L to the values of 130 nF and 20 mH, respectively. A fine tuning of the inductance L from 20 mH to 21.5 mH, and of the capacitance L from 130 nF to 133 nF, brings f_{Chua} to about 1810 Hz, whereas f_{plasma} is kept at the constant value of 1760 Hz (Fig. 2). As we shall see, this mismatch of about 50 Hz between f_{Chua} and f_{plasma} for the uncoupled oscillators ($R_c\rightarrow\infty$) is not large enough to prevent the onset of phase synchronization when the coupling is turned on.

Simultaneously with the power spectra, while the two oscillators are still uncoupled, we plot on the real-time scope the plasma light intensity signal versus the Chua signal. An ellipselike figure oscillates back-and-forth around its center, sometimes tilted to the right sometimes tilted to the left, as depicted in Fig. 3. The back-and-forth oscillations happen due to the 2π phase slips between plasma and Chua. These phase slips do not happen instantaneously, rather the two oscillators may go around a few cycles before their phases get much far apart from each other, and eventually catch up again after a full 2π phase difference. One of the oscillators goes faster than the other and the phase difference grows until the faster oscillator has gone a full cycle ahead. Therefore the back-and-forth oscillations of the ellipse on the scope. We proceed with the tuning described in the preceding paragraph, and notice that the back-and-forth oscillations of the ellipse slows down as f_{Chua} approaches f_{plasma}. When the mismatch between these two frequencies is about 50 Hz, the back-and-forth oscillation of the ellipse is reduced to a minimum. At this point, with R_c set at 0.7 $\text{K}\Omega$, we switch the coupling connection on and observe a sudden shift of the peak of the plasma spectrum toward the peak position of the Chua spectrum. As shown in Fig. 4, the coupled oscillators are now running with the same characteristic frequency $f_{\text{Chua}}=f_{\text{plasma}}=1810$ Hz. For this specific value, our recording capability allows the checking for phase synchronization over 23 710 consecutive cycles of oscillation, with an average sampling of 11 points per cycle. The ellipse plotted on the scope, and depicted in Fig. 5, becomes stable with no back-and-forth oscillations. It remains stable for long time

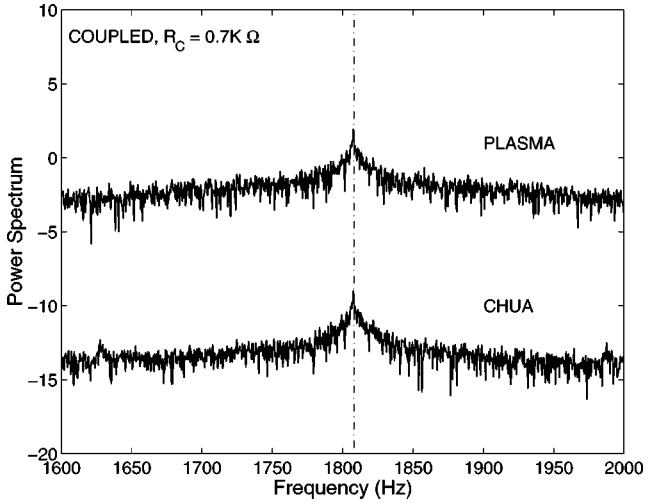

FIG. 4. Power spectra of the coupled plasma and of the Chua oscillator. The two dominant frequencies match.

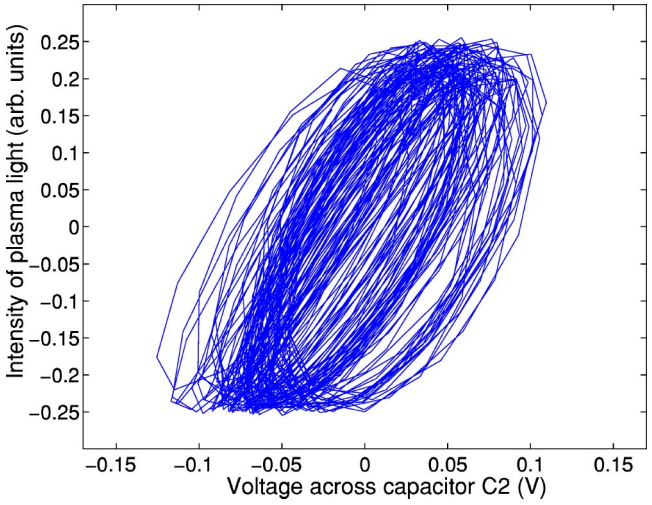

FIG. 5. Plot of the voltage across capacitor C_2 of the Chua circuit vs the light intensity of the plasma discharge when the two oscillators are coupled.

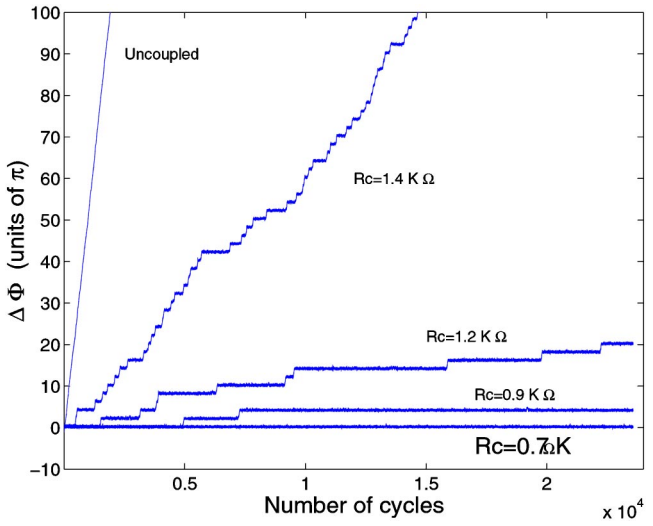

FIG. 6. Time evolution of the phase difference between the phase of Chua circuit and the phase of the plasma $\Delta\phi=\phi_{\mathrm{Chua}}-\phi_{\mathrm{plasma}}$ for several values of the coupling resistance R_c, as indicated.

intervals, a clear indication of a robust phase synchronized state between the plasma and the Chua oscillator. The amplitudes of the two oscillators remain uncorrelated but their phases are now in step with each other. There is a small phase difference but this difference $\Delta\phi=\phi_{\mathrm{Chua}}-\phi_{\mathrm{plasma}}$ does not grow in time. It remains small and bounded within an angle less than 2π.

Next we vary the coupling resistance R_c in order to measure the effect of different coupling strengths. We notice that the phase synchronous state is more robust for lower values of R_c (which means stronger coupling). In this case, long periods of phase synchronization are observed in real time with the stable ellipse plotted on the scope. However, as we increase the value of R_c, therefore weakening the coupling, we observe intermittent oscillation bursts of the ellipse on the scope. These bursts occur at irregular time intervals and correspond to slips of 2π in the phase difference $\Delta\phi$, confirmed when we analyze the data acquired in the computer. The bursts become more frequent with the further lowering of the coupling strength, as demonstrated in Fig. 6, which clearly shows the overall decrease in the average time between 2π slips as the coupling strength is lowered. These 2π slips have been observed numerically [2] and experimentally [6], and identified in both cases with chaotic transients [8]. Chaotic transients have been extensively investigated in association with unstable-unstable pair bifurcations where two unstable periodic orbits of the same period coalesce and disappear as a system parameter is raised [9]. Approaching the bifurcation from above, i.e., increasing the coupling strength, the average length of the chaotic transient diverges, and below the critical value of the coupling bifurcation parameter, the chaotic transient may be regarded as converted into a chaotic attractor. Typically, long chaotic transients persist even for parameter values relatively far from the bifurcation point. This is experimentally relevant because, for the duration of the measurement, long-lived chaotic transients may prevent the system from reaching the time asymptotic state. In the second paper of Ref. [6], experimental chaotic phase synchronization has been observed to be superpersistent transient, following the scaling law $\tau\sim\exp[A(p-p_c)^{\beta}]$, with $p>p_c$, where $A>0$ is a constant, $\beta>0$ is the scaling exponent, and p_c is the critical parameter value for the coupling strength p. In this Ref. [6], chaotic transient is observed to happen due to the influence of additive noise. That is not the case in our present experimental study. Here, even though the intrinsic presence of noise in the experimental setup is unquestionable, we observe transient chaos in association with the strength of the coupling parameter between the two systems. We run the experiment many times with different values for the coupling resistance. For each value, a total of 20 data sets are acquired in order to compute the mean time interval for sustained phase synchronization between consecutive phase slips of 2π. These measurements show that the mean time τ between the phase slips obeys the

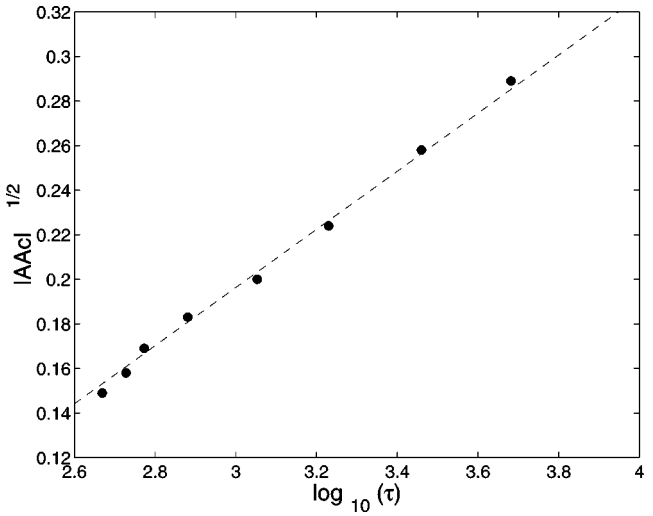

FIG. 7. Scaling of the chaotic transient where τ is the average transient time and $A_c=1/80$.

scaling $\ln,\tau \sim \text{const} \times |R - R_{crit}|^{-1/2}$, where $R_{crit} \approx 1000\Omega$ is the critical value of the coupling resistance. This result is in agreement with the numerical results for flows [2] and maps [8], and is also consistent with the unstable-unstable pair bifurcation crisis theory [9]. Furthermore, it is consistent with our numerical simulation of the plasma circuit coupled to the Chua oscillator which is described in the following paragraph.

Model equations for the plasma circuit can be obtained by treating the plasma discharge as a nonlinear component, with a piecewise linear voltage-current characteristic. We apply Kirchoff's laws to the plasma circuit only and get (see Ref. [4] for details) $\dot{x} = \alpha E/R - \alpha(x-y) - V_P(x)\alpha/R$, $\dot{y} = x - y + z + \mathrm{A}v_{C_2}$, and $\dot{z} = -\beta y$. Here, x, y, and z are related to the currents and voltages in the circuit, with parameter values $\alpha = 8.0$, $E = 850$, $R = 30\,000$, and $\beta = 10.2$. $V_P(x)$ represents a piecewise linear resistor [10], and Av_{C_2} is the input coming from the numerical solution of the Chua equations [7]. The factor A corresponds to the coupling strength, analogous to the variable resistor R_c of the experimental setup displayed in Fig. 1, and v_{C_2} is the voltage across capacitor C_2 in the Chua system [7]. This is a straightforward coupling where the output of a system is directly introduced into another through a coupling resistance. The incoming Chua signal is multiplied by a reducing factor $(0 < A < 1)$ in order to control its amplitude. For small values of A, the incoming Chua signal can be viewed as a small chaotic perturbation that forces phase synchronization between plasma and Chua. Different values of A produce different levels of coupling, with extended times of phase synchronized states intercalated with short bursts of 2π phase slips between plasma and Chua. Here too, the mean time τ between phase slips obeys the scaling $\ln \tau \sim \text{const} \times |A - A_{crit}|^{-1/2}$, as shown in Fig. 7. It clearly demonstrates that the statistics of the phase slips corresponds to the statistics of Poincaré recurrence times for a chaotic system.

The experimental technique presented here for the implementation of phase synchronization between two different chaotic systems incorporates a real-time control and detection approach that is invaluable for the optimization of the process. We expect it to be relevant in a variety of fields including plasmas, laser, electrochemistry, fluids, and engineering applications in general.

[1] M.G. Rosenblum, A.S. Pikovsky, and J. Kurths, Phys. Rev. Lett. **76**, 1804 (1996); A.S. Pikovsky, M.G. Rosenblum, and J. Kurths, *Synchronization: A Universal Concept in Nonlinear Science*, 2nd ed. (Cambridge University Press, Cambridge, 2003).

[2] E. Rosa, Jr., E. Ott, and M.H. Hess, Phys. Rev. Lett. **80**, 1642 (1998); R. Breban and E. Ott, Phys. Rev. E **65**, 056219 (2002).

[3] U. Parlitz, L. Junge, W. Lauterborn, and L. Kocarev, Phys. Rev. E **54**, 2115 (1996); P.M. Varangis, A. Gavrielides, T. Erneus, V. Kovanis, and L.F. Lester, Phys. Rev. Lett. **78**, 2353 (1997); J.R. Terry, K.S. Thornburg, Jr., D.J. DeShazer, G.D. VanWiggeren, S. Zhu, P. Ashwin, and R. Roy, Phys. Rev. E **59**, 4036 (1999); A. Neiman, X. Pei, D. Russell, W. Wojtenek, L. Wilkens, F. Moss, H.A. Braun, M.T. Huber, and K. Voigt, Phys. Rev. Lett. **82**, 660 (1999); G.M. Hall, S. Bahar, and D.J. Gauthier, *ibid.* **82**, 2995 (1999); Z. Zheng, G. Hu, and B. Hu, Phys. Rev. E **62**, 7501 (2000); D.J. DeShazer, R. Breban, E. Ott, and R. Roy, Phys. Rev. Lett. **87**, 044101 (2001); K. Josic and D.J. Mar, Phys. Rev. E **64**, 056234 (2001); C. Zhou, J. Kurths, I.Z. Kiss, and J.L. Hudson, Phys. Rev. Lett. **89**, 014101 (2002); D.L. Valladares, S. Boccaletti, F. Feudel, and J. Kurths, Phys. Rev. E **65**, 055208 (2002); M.A. Zaks, E.-H. Park, and J. Kurths, *ibid.* **65**, 026212 (2002); I. Tokuda, J. Kurths, and E. Rosa, Jr., Phys. Rev. Lett. **88**, 014101 (2002).

[4] C.M. Ticos, E. Rosa, Jr., W.B. Pardo, J.A. Walkenstein, and M. Monti, Phys. Rev. Lett. **85**, 2929 (2000).

[5] W.B. Pardo, E. Rosa, Jr., C.M. Ticos, J.A. Walkenstein, and M. Monti, Phys. Lett. A **284**, 259 (2001).

[6] A.S. Pikovsky, M.G. Rosenblum, G.V. Osipov, and J. Kurths, Physica D **104**, 219 (1997); L. Zhu, A. Raghu, and Y.-C. Lai, Phys. Rev. Lett. **86**, 4017 (2001).

[7] M.P. Kennedy, Frequenz **46**, 66 (1992).

[8] A. Pikovsky, G. Osipov, M. Rosenblum, M. Zaks, and J. Kurths, Phys. Rev. Lett. **79**, 47 (1997).

[9] C. Grebogi, E. Ott, and J.A. Yorke, Ergod. Theory Dyn. Syst. **5**, 341 (1985); Phys. Rev. Lett. **50**, 935 (1983).

[10] The $V_P(x)$ piecewise linear function used in this simulation contains one more slope in addition to the two slopes of the function presented in Ref. [4]. Here, $V_P(x) = 0$ for $x < 0$, $V_P(x) = 109x + 160$ for $0 \leqslant x < 0.73$, $V_P(x) = -36.4x + 267$ for $0.73 \leqslant x < 2.6$ $V_P(x) = -2x + 177$ for $2.6 \leqslant x$. More details about our simulation and model equations to come in a future publication.